

Photostimulated luminescence from $\text{BaCl}_2:\text{Eu}^{2+}$ nanocrystals in lithium borate glasses following neutron irradiation

G. A. Appleby^{a)} and A. Edgar

MacDiarmid Institute, Victoria University of Wellington, P.O. Box 600, Wellington, New Zealand

G. V. M. Williams

Industrial Research Limited, Wellington, New Zealand and MacDiarmid Institute, Victoria University of Wellington, P.O. Box 600 Wellington, New Zealand

A. J. J. Bos

Faculty of Applied Sciences, Delft University of Technology, 2629 JB Delft, The Netherlands

(Received 20 February 2006; accepted 25 June 2006; published online 5 September 2006)

A glass-ceramic thermal neutron imaging plate material is reported. The material consists of a neutron sensitive $2\text{B}_2\text{O}_3\text{-Li}_2\text{O}$ glass matrix containing nanocrystallites of the storage phosphor $\text{BaCl}_2:\text{Eu}^{2+}$. When doped with 0.5 mol % Eu^{2+} , the neutron induced photostimulated luminescence (PSL) conversion efficiency of the ^{10}B enriched glass-ceramic is around 60% of that a commercial neutron imaging plate, while the γ sensitivity is an order of magnitude lower than that of the commercial plate. A Eu^{2+} -concentration series shows that the PSL efficiency for x rays is optimized at 0.01 mol % Eu^{2+} . Thermoluminescence measurements indicate trap depths in $\text{BaCl}_2:\text{Eu}^{2+}$ ranging from 0.55 to 2.7 eV. © 2006 American Institute of Physics. [DOI: 10.1063/1.2335807]

Thermal neutron radiography is a powerful method of imaging internal structure and provides a complimentary image to standard x ray imaging. While x-rays are attenuated by elements with high atomic number, for thermal neutrons the reverse is generally true, resulting in radiographs which show the distribution of light elements, such as hydrogen, within an object. A detailed overview is given by Lehmann *et al.*¹

Commercially available neutron imaging plates (NIPs) from Fujifilm contain a powder mix of Gd_2O_3 and $\text{BaFBr}:\text{Eu}^{2+}$ in a polymer binder on a supporting layer.² The ionizing radiation emitted from the Gd neutron capture reactions generates electron hole pairs in the storage phosphor $\text{BaFBr}:\text{Eu}^{2+}$, which are trapped in stable electron and hole centers. The spatial variation of these trapped charge carriers (F centers in the case of electrons) represents a latent image of the object of interest. The image is read out by stimulating electron-hole recombination with a scanned red or green laser where the recombination energy is transferred to a Eu^{2+} ion, and appears as photostimulated luminescence (PSL).³

However, the use of the high Z elements Gd, Ba, and Br in Fuji's NIP results in a high sensitivity to the broad γ -radiation background present in neutron experiments. A further problem is the scattering of the stimulating readout light by powder grains within the NIP, resulting in poor spatial resolution.

Glass-ceramics NIP can potentially have a significantly better spatial resolution. In the case of x-ray storage phosphors, it was shown by Edgar *et al.*⁴ that the spatial resolution of fluorozirconate glass-ceramics containing nanocrystalline orthorhombic $\text{BaCl}_2:\text{Eu}^{2+}$ is much better than that of commercial x-ray imaging plates composed of powdered $\text{BaFBr}:\text{Eu}^{2+}$ in an organic binder.

In this letter we report the discovery of a glass-ceramic NIP material which has high sensitivity to thermal neutrons and a low sensitivity to γ radiation. The NIP material consists of nanocrystallites of orthorhombic $\text{BaCl}_2:\text{Eu}^{2+}$ suspended in a neutron sensitive lithium borate glass matrix. Thermal neutron detection occurs via the $^{10}\text{B}(n, \alpha)^7\text{Li}$ and $^6\text{Li}(n, \alpha)^3\text{H}$ reactions (thermal neutron capture cross sections of $\sigma=3838$ and 941 b, respectively), which give rise to secondary alpha particle energy resulting in electron-hole pair generation and F -center formation in the storage phosphor nanocrystallites. The neutron image can be read out with commercial imaging plate readout scanners.

This glass-ceramic NIP is expected to possess considerable advantages over the Fuji NIP, such as reduced scattering for improved spatial resolution, a lower effective atomic number for reduced γ sensitivity, and the ability to be molded into arbitrary shapes, such as optical fiber sensors.

A previous study of the γ sensitivity of a glass ceramic of composition $59\text{B}_2\text{O}_3\text{-}29\text{Li}_2\text{O}\text{-}12\text{BaCl}_2$ has found that these materials have much lower γ sensitivity than the Fuji BAS-ND over a range of γ energies from 15 to 660 keV.⁵

The composition of the NIP material was $56.7\text{B}_2\text{O}_3\text{-}25.8\text{Li}_2\text{O}\text{-}2.5(2\text{LiF})\text{-}15\text{BaCl}_2:\text{Eu}^{2+}$. The glasses were doped with 0.005–0.5 mol % EuCl_2 as a luminescence center, and 4 mol% SiO_2 to minimize the problem of hygroscopy in $2\text{B}_2\text{O}_3\text{-Li}_2\text{O}$ glass.⁶ A previous study has shown that fluoride doping in halide storage phosphors enhances PSL significantly, so in these materials 2.5 mol% Li_2O was replaced with 2.5 mol% 2LiF to enhance the PSL.⁷

The B_2O_3 was dried at 500 °C for 1 h in a Pt crucible in an Ar atmosphere. The remaining powders were added in a N_2 atmosphere and melted at 1000 °C for 1 h in Ar. The melt was poured onto a Cu quenching block held at 300 °C and cooled to room temperature. Samples were subsequently annealed at 540 °C to promote crystal growth.

X-ray powder diffraction (XRD) was performed using a Philips diffractometer with a Cu tube operated at 40 kV and

^{a)} Author to whom correspondence should be addressed; electronic mail: gappleby@paradise.net.nz

35 mA. The mean particle size was estimated from the XRD line widths using the Scherrer formula.⁸

A Perkin-Elmer LS-55 luminescence spectrometer was used to measure the photoluminescence (PL) and PSL spectra of each sample. For low energy x-ray induced PSL measurements, samples were irradiated for 30 s with x rays at room temperature using a Philips PW1720 x-ray generator with an Al-filtered W tube operated at 50 kV and 20 mA. The PSL conversion efficiency (CE) was measured using a custom-made PSL detector. It is defined as the PSL output per incident absorbed dose.

Thermoluminescence (TL) of samples containing 0.5 mol % Eu^{2+} was measured using a Risø-TL/PSL-DA-15A/B reader, with an installed $^{90}\text{Sr}/^{90}\text{Y}$ β source with a dose rate of 1 mGy/s in air. Measurements were made following β irradiation with doses of 30–3840 mGy. A temperature ramp rate of 1 K/s was used from room temperature to 400 °C.

Neutron irradiation was performed using one of the beamlines of the IRI nuclear research reactor in Delft, The Netherlands. 1 mm thick samples containing 0.5 mol % Eu^{2+} were exposed for 30 s to the neutron flux, measured to be around $1 \times 10^5 \text{ cm}^{-2} \text{ s}^{-1}$. PSL was measured with a Risø TL-DA-15B/C reader with a green ($550 \pm 25 \text{ nm}$) lamp as stimulation source and a 9235QA photomultiplier tube, shielded by 5 mm BG-4+2 mm BG-37 Schott filters, as detector. Following irradiation, the CE was measured by integrating the total PSL light output during constant photostimulation. The CE of the glass-ceramics for both neutron and x irradiation were computed with respect to a sample of the Fuji NIP BAS-ND irradiated under the same conditions. The stimulation energy (SE) of the glass-ceramic has been obtained by measuring the photostimulation time required for the PSL intensity to decrease to $1/e$ of its initial value, and compared with that of the BAS-ND material.

The unannealed material is an opaque white glass-ceramic and XRD shows that it contains nanocrystalline orthorhombic BaCl_2 . Annealing at 540 °C for 10 min does not change the visual appearance of the material; however, the XRD patterns show that upon annealing the crystallites grow in size from ~ 60 to 86 nm. The volume fraction of the crystals also increases significantly upon annealing which is evident from the increase in relative intensity of the BaCl_2 diffraction peaks to the glassy background.

When excited with 270 nm light, the glass-ceramics show PL at 401 nm (Fig. 1). This is the characteristic emission of orthorhombic $\text{BaCl}_2:\text{Eu}^{2+}$.⁹ The glass-ceramics show PSL upon x-ray irradiation and the PSL emission and excitation spectra are also shown in Fig. 1. It can be seen that the luminescent center responsible for the 401 nm PL emission is PSL active. Orthorhombic BaCl_2 has two inequivalent Cl sites (of C_2 point symmetry) where the excited $2p$ state of the related F center can be split into three levels. The PSL excitation spectrum contains three peaks (at 433, 502, and 671 nm), for which the simplest explanation is that only a single Cl site is PSL active. To investigate this, the PSL excitation measurement is repeated having photostimulated the irradiated sample with 671 nm light. It was found that the only effect of this is to reduce the intensity of the whole spectrum, rather than just the peak at 671 nm. This indicates that PSL from orthorhombic $\text{BaCl}_2:\text{Eu}^{2+}$ in these glass-ceramics arises from just one F center, which is split into three bands.

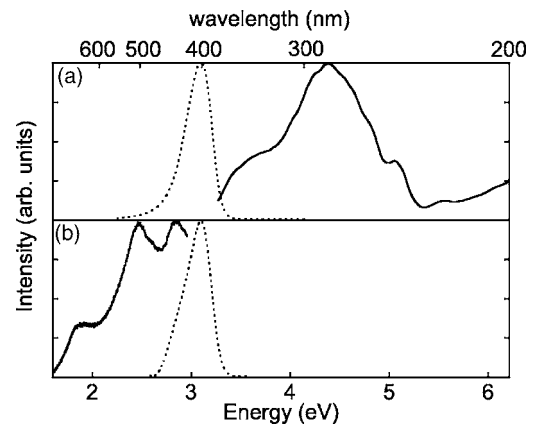


FIG. 1. (a) Normalized photoluminescence emission spectra, excited at 270 nm, of a $56.7\text{B}_2\text{O}_3-25.8\text{Li}_2\text{O}-2.5(2\text{LiF})-15\text{BaCl}_2:\text{Eu}^{2+}$ ($\text{Eu}^{2+}=0.5 \text{ mol } \%$) glass-ceramic annealed at 540 °C for 10 min (dotted curve) and excitation spectra detected at 401 nm (solid curve). (b) Normalized PSL emission spectra, excited at 520 nm, of the same glass-ceramic (dotted curve) and PSL excitation spectra detected at 380 nm (solid curve). All spectra were recorded at room temperature.

The TL glow curve from a glass-ceramic following a dose of 120 mGy β irradiation is shown in Fig. 2. The glow curve was fitted using the Weibull distribution function,¹⁰ and contains five glow peaks at 365, 392, 470, 501, and 667 K with trap depths of 0.87, 0.55, 0.58, 1.2, and 2.7 eV, respectively. The trap depths were calculated by fitting to the glow curve a function based on the Weibull distribution as described by Pagonis *et al.*¹⁰ The dose dependence of the peaks and their sum are also shown in Fig. 2. There is a slight deviation from linearity of the 365 K peak (peak 1) at high dose, indicating that these traps have been saturated at a dose of 3840 mGy. Additionally, the high temperature peak at 667 K (peak 5) seems to show a sublinear response at low dose. However, as these sublinear peaks are relatively low in intensity, the overall TL response is close to linear.

To investigate which of the TL traps are active in PSL, the glow curve was measured following exposure of the x-ray-irradiated material to red stimulating light. The resulting glow curve consisted of only peak 2. This indicates that peaks 1, 3, and 4 are photostimulable and may be related to

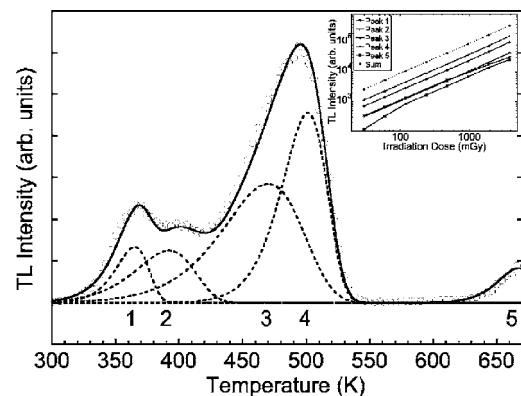


FIG. 2. Thermoluminescence glow curve following a dose of 120 mGy of β irradiation of a $56.7\text{B}_2\text{O}_3-25.8\text{Li}_2\text{O}-2.5(2\text{LiF})-15\text{BaCl}_2:\text{Eu}^{2+}$ ($\text{Eu}^{2+}=0.5 \text{ mol } \%$) glass-ceramic annealed at 540 °C for 10 min (open symbols); five numbered peaks fitted to the glow curve using the Weibull function (dashed line); the sum of the individual Weibull functions (solid line). The heating rate is 1 K/s. Inset: the dependence of each Weibull function peak intensity on radiation dose (solid line) and the sum of the Weibull function peak intensities (dashed line).

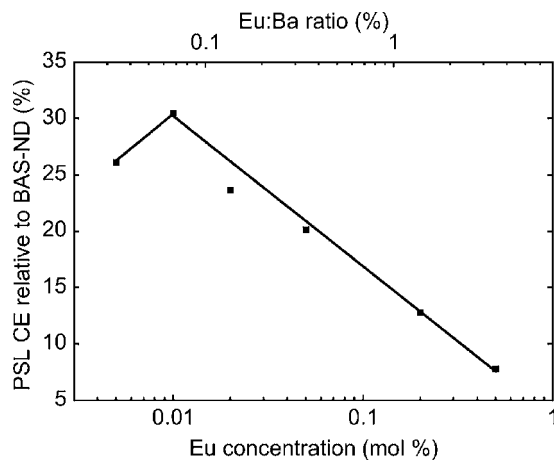


FIG. 3. PSL conversion efficiency of $56.7\text{B}_2\text{O}_3-25.8\text{Li}_2\text{O}-2.5(2\text{LiF})-15\text{BaCl}_2:\text{Eu}^{2+}$ glass-ceramics annealed at 540°C for 10 min, as a function of Eu^{2+} content. The line is a guide for the eyes.

the three peaks in the PSL excitation spectrum, while peak 2 is not active in PSL. Peak 5 did not appear in the x-ray induced glow curve which suggests that it is a β -induced trap.

Following thermal neutron irradiation, the glass-ceramics show strong PSL. The PSL conversion efficiency for a sample containing natural B and Li is around 15% of that of the Fuji NIP, while for a sample enriched with 99% ^{10}B , the CE is close to 60%. This shows that the PSL is due to thermal neutrons, rather than γ irradiation. The CE increase is due to the half thickness to thermal neutrons of the material decreasing from 4.25 to 0.90 mm upon ^{10}B enrichment. It is likely that this CE will increase further upon enrichment with ^6Li . The time required for the PSL signal to drop to $1/e$ of its initial value in these measurements was 0.69 s for the ^{10}B -enriched glass-ceramic and 0.54 s for the BAS-ND. Thus, the SE of the glass-ceramic is about 1.3 times larger than the BAS-ND material but this is not a serious limitation in the practical use.

Figure 3 shows the dependence of x-ray induced PSL in the glass-ceramics on Eu^{2+} content. The glass-ceramics show much weaker PSL than the Fuji NIP when exposed to x rays over a range of Eu concentrations, which has a maximum of 30% at 0.01 mol % Eu^{2+} . It should be noted that the neutron induced PSL was measured using a glass-ceramic containing 0.5 mol % Eu^{2+} . This material has an x-ray induced PSL CE of only 7% of that of the Fuji NIP. The glass-ceramic is therefore a NIP material with a high neutron sensitivity combined with a very good neutron to γ discrimination.

Figure 3 also shows that the PSL CE at 0.01 mol % Eu^{2+} is more than four times greater than that at 0.5 mol % Eu^{2+} . As the neutron induced PSL can be expected to scale with x-ray induced PSL in this series, it is possible that the glass-ceramic NIPs can be optimized to have higher sensitivity to thermal neutrons than the BAS-ND.

An initial increase of PSL with Eu concentration followed by a decrease due to concentration quenching is a phenomenon that has been observed in other materials. Hackenschmied *et al.*¹¹ have shown that the x-ray-radiation induced PSL CE in $\text{BaFBr}:\text{Eu}^{2+}$ is dependent on the Eu^{2+} content where the CE is optimized when this concentration is 0.1 mol % and decreases significantly as the Eu content in-

creases. In the glass ceramics, the CE is maximized at an Eu:Ba ratio of 0.07% which is close to that of $\text{BaFBr}:\text{Eu}^{2+}$.

An important consideration when developing neutron detectors is the possible neutron capture by atoms other than the principal neutron converter. This can sometimes result in the formation of radioactive nuclei, which will decay with the emission of characteristic β and/or γ radiation. This leads to the generation of weak background PSL in an imaging plate, as well as posing a potential health risk. In the BAS-ND, the isotopes that are activated are ^{79}Br , ^{81}Br , and ^{151}Eu , each of which has a relatively high thermal neutron capture cross section and forms unstable nuclei on neutron capture. It takes 75 h before the radiation level is below an acceptable level.² The replacement of Br by Cl partially eliminates this problem in the glass-ceramics. ^{35}Cl is likely to form the radioactive ^{36}Cl upon neutron capture; however, the half life of the decay is 3×10^5 yr, so this is unlikely to be a problem.

The Eu content in the glass-ceramics results in radioactivity with a half life of 550 min, so that the glass-ceramics become radioactive for 2–3 days after neutron irradiation. The particular samples exposed to neutrons contained a relatively high Eu content, 0.5 mol %, which led to background PSL in subsequent measurements so the glass-ceramics had to be thermally bleached at 350°C prior to each PSL measurement. Reduction of Eu concentration in the glass-ceramics to 0.01 mol % will therefore result in significant reduction in neutron activation as well as an improved PSL CE. Another possible solution to the problem of activation is to replace Eu^{2+} with Ce^{3+} which is known to exhibit PSL in $\text{BaCl}_2:\text{Ce}^{3+}$ crystals.¹² Ce ($\sigma=0.63$ b) has a much lower neutron capture cross section than Eu ($\sigma=4600$ b).

The glass-ceramics reported in this letter are opaque because of optical scattering from the BaCl_2 crystallites. This will limit the spatial resolution when these materials are used in thermal neutron imaging plates. However, we expect an improved spatial resolution if the glass-ceramics can be prepared in transparent or translucent form.^{4,13}

The authors thank the New Zealand Foundation for Research Science and Technology for financial support.

¹E. H. Lehmann, P. Vontobel, G. Frei, and C. Brönimann, Nucl. Instrum. Methods Phys. Res. A **531**, 228 (2004).

²S. Tazaki, K. Neriishi, K. Takahashi, M. Etoh, Y. Karasawa, S. Kumazawa, and N. Niimura, Nucl. Instrum. Methods Phys. Res. A **424**, 20 (1999).

³S. Schweizer, Phys. Status Solidi A **187**, 335 (2001).

⁴A. Edgar, G. V. M. Williams, S. Schweizer, and J.-M. Spaeth, Curr. Appl. Phys. **6**, 399 (2006).

⁵G. A. Appleby, C. M. Bartle, G. V. M. Williams, and A. Edgar, Curr. Appl. Phys. **6**, 389 (2006).

⁶T. W. Donald, B. L. Metcalfe, D. J. Bradley, M. J. C. Hill, and J. L. McGrath, J. Mater. Sci. **29**, 6379 (1994).

⁷G. A. Appleby, A. Edgar, and G. V. M. Williams, J. Appl. Phys. **96**, 6281 (2004).

⁸H. P. Klug and L. E. Alexander, *X-Ray Diffraction Procedures*, 2nd ed. (Wiley, New York, 1974), Chap. 9, p. 491.

⁹M. Secu, R. Kalchgruber, S. Schweizer, J.-M. Spaeth, and E. Edgar, Radiat. Eff. Defects Solids **157**, 957 (2002).

¹⁰V. Pagonis, S. M. Mian, and G. Kitis, Radiat. Prot. Dosim. **93**, 11 (2001).

¹¹P. Hackenschmied, H. Li, E. Epelbaum, R. Fastbender, M. Batenschuk, and A. Winnacker, Radiat. Meas. **33**, 669 (2001).

¹²J. Selling, S. Schweizer, J.-M. Spaeth, G. Corradi, A. Edgar, and G. V. M. Williams, Phys. Status Solidi C **2**, 592 (2005).

¹³G. Chen, J. Johnson, R. Weber, R. Nishikawa, S. Schweizer, P. Newman, and D. MacFarlane, J. Non-Cryst. Solids **352**, 610 (2006).